

Effect of cooling rate on shear bond strength of veneering porcelain to a zirconia ceramic material

Futoshi Komine^{1,2}), Ayako Saito³), Kazuhisa Kobayashi¹), Mai Koizuka³),
Hiroyasu Koizumi^{1,2}) and Hideo Matsumura^{1,2})

¹)Department of Fixed Prosthodontics, Nihon University School of Dentistry, Tokyo, Japan

²)Division of Advanced Dental Treatment, Dental Research Center, Nihon University School of Dentistry, Tokyo, Japan

³)Division of Applied Oral Sciences, Nihon University Graduate School of Dentistry, Tokyo, Japan

(Received 20 October and accepted 15 November 2010)

Abstract: The purpose of the present study was to evaluate the effect of cooling rates after firing procedures of veneering porcelain on shear bond strength between veneering porcelain and a zirconium dioxide (zirconia; ZrO₂) ceramic material. A total of 48 ZrO₂ disks were divided equally into three groups. Two veneering porcelains that are recommended for ZrO₂ material – Cerabien ZR (CZR), IPS e.max Ceram (EMX) – and one that is recommended for metal ceramics – Super Porcelain AAA (AAA) were assessed. Each group was then further divided into two subgroups ($n = 8$) according to cooling time (0 or 4 min) after porcelain firing. Specimens were fabricated by veneering the porcelain on the ZrO₂ disks, after which shear bond testing was conducted. Bond strength differed significantly by cooling time in ZrO₂-AAA ($P < 0.001$) and ZrO₂-EMX ($P = 0.001$) specimens. There was no significant difference in shear bond strength with respect to cooling time in ZrO₂-CZR specimens ($P = 0.382$). The duration of cooling from firing temperature to room temperature may affect the shear bond strength of veneering porcelain to a zirconia material depending on porcelain material used. (J Oral Sci 52, 647-652, 2010)

Keywords: bond strength; cooling rate; veneering porcelain; zirconia.

Introduction

Dental porcelain is one of the most esthetically appealing synthetic materials for replacement of missing teeth. Favorable esthetic results in restorative treatments can be achieved by using dental porcelain materials that mimic the optical properties and appearance of natural teeth. Due to the brittleness and limited tensile strength of veneering porcelain, the methods used to combine strong core materials, such as metal, with porcelain materials have continued to be refined over a period of many decades. The recent increase in demand for esthetic restorations has led to greater use of all-ceramic core materials, owing to their superior esthetics and biocompatibility as compared with metal-ceramic systems (1,2).

With the development of computer-aided design/computer-aided manufacturing (CAD/CAM) in dentistry, zirconium dioxide (zirconia; ZrO₂) ceramic materials have been introduced and widely applied in fixed restorations. Short- and medium-term clinical studies (3-6) of zirconia-based fixed restorations showed that zirconia ceramics were highly stable as a framework material. However, minor chipping of the veneering porcelain was described as the most frequent complication resulting in failure of zirconia-based restorations. Chipping rates were reported to be 15% at 24 months (3), 25% at 31 months (4), and 15% at 53 months (5). Studies have indicated that mechanical retention and bonding of the veneering porcelain to the

framework material are key factors in the successful performance of veneer-framework bilayered restorations (4,7).

Fracture of porcelain usually progresses from the area that is subjected to the highest tensile stress. Microcracks and porosities progressing from the inner surface can increase internal stress in bilayered restorations and ultimately result in damage to these restorations (8). Initial cracks have been observed under the following conditions: mismatch of coefficient of thermal expansion (CTE) between the veneering porcelain and framework material, firing shrinkage of the porcelain, improper fabrication of the restorations during grinding or other machining, and undesirable heating and cooling rates (7,9). Tuccillo and Nielsen (10) suggested that the rate at which the veneering porcelain/metal framework composite cools from the firing temperature of the porcelain may be related to shear stresses that are sufficient to affect adversely the bond strength between veneering porcelain and the metal framework. Residual stresses at the boundary of the veneering porcelain/metal framework composite depend on the thermal history of porcelain firing (11). Furthermore, controlled cooling rates might enhance the bond strength of veneering porcelain to the metal framework (10,12). An *in vitro* study (13) of the influence of cooling rate on the bond strength between a zirconia core material and veneering porcelain indicated that bond strength was reduced by slow cooling. However, there are few data on the effect of cooling rates on the bond strength of veneering porcelain to zirconia material. The objective of the present study, therefore, was to evaluate the effect of cooling rates after firing procedures of veneering porcelain on shear bond strength between veneering porcelain and a zirconia ceramic material.

Materials and Methods

Table 1 shows the substrate and veneering porcelains

investigated in the present study. A total of 48 ZrO₂ disks were fabricated with the Katana system (Noritake Dental Supply Co., Ltd., Miyoshi, Japan) as substrates for bonding. To fabricate ZrO₂ substrates, the presintered ZrO₂ blanks (Katana Zirconia, Noritake Dental Supply Co., Ltd.) were milled with Katana H-18 (Noritake Dental Supply Co., Ltd.) and sintered to full density in a furnace (Katana F-1, Noritake Dental Supply Co., Ltd.) at 1400°C for 90 min. The ZrO₂ substrate was formed into a disk (11.0 mm in diameter and 2.7 mm thick). The surfaces of substrates were wet-ground with 600-grit silicon carbide paper (Tri-M-ite Wetordry sheets, 3M ESPE, St. Paul, MN, USA), followed by airborne particle abrasion with 50- μ m alumina (Hi-Aluminas, Shofu Inc., Kyoto, Japan) at a pressure of 0.2 MPa from a distance of 10 mm and, finally, ultrasonic cleaning with acetone for 10 min (Ultrasonic Cleaner SUC-110, Shofu Inc.).

The specimens were divided into three groups, and two veneering porcelains recommended for ZrO₂ material and one recommended for metal ceramics were assessed: Cerabien ZR (CZR, Noritake Dental Supply Co., Ltd.), IPS e.max Ceram (EMX, Ivoclar Vivadent AG, Schaan, Liechtenstein), and Super Porcelain AAA (AAA, Noritake Dental Supply Co., Ltd.). Each group was further divided into two subgroups ($n = 8$) according to cooling time after porcelain firing (0 or 4 min). The manufacturer's recommended cooling time is 0 min for AAA and EMX and 4 min for CZR (Table 2). Specimens with a cooling time of 0 min were immediately removed from the furnace and cooled in ambient air. Specimens with a cooling time of 4 min were cooled from the sintering temperature, outside the furnace, for 4 min. All specimens were cooled from firing temperature to glass transition temperature (T_g).

The veneering area was determined by using a piece of plastic tape (Star Traper-GP, Sakurai Co., Tokyo, Japan) with a 5-mm-diameter circular hole on the substrates.

Table 1 Materials investigated in the present study

Material (Brand name)	Code	Manufacturer	Lot No.	Composition	CTE*
Zirconia ceramic					
Katana Zirconia	ZrO ₂	Noritake Dental Supply Co., Ltd., Miyoshi, Japan	200218	94.4% ZrO ₂ , 5.4% Y ₂ O ₃	10.5
Feldspathic porcelain for gold alloy					
Super Porcelain AAA	AAA	Noritake Dental Supply Co., Ltd.	18236	Body A3B	12.4
Feldspathic porcelain for zirconia					
Cerabien ZR	CZR	Noritake Dental Supply Co., Ltd.	18206	Body A3B	9.1
IPS e.max Ceram	EMX	Ivoclar Vivadent AG, Schaan, Liechtenstein	L09526	Dentin/Body A-D Shades A3	9.5

* Coefficient of thermal expansion (CTE) in $\times 10^{-6} \text{ } ^\circ\text{C}^{-1}$ between 25°C and 500°C.

Table 2 Firing schedules for veneering porcelains (based on manufacturers' recommendations)

Veneering porcelain	Predrying temperature (°C)	Time (min)	Heating rate, firing (°C/min)	Temperature (°C)	Holding time (min)	Cooling time (min)
AAA	600	7	45	920	0	0
CZR	600	7	45	940	1	4
EMX	403	4	50	750	1	0

See Table 1 for description of abbreviations.

Veneering porcelain slurry was placed on the veneering area and condensed with ultrasonic agitation using the Ceracon II (Shofu Inc.). Firing was performed in a porcelain furnace (Single Mat, Shofu Inc.), after which the porcelain slurry was layered on the specimens with a specially designed polytetrafluoroethylene (PTFE) split mold (K826, Tokyogiken Inc., Tokyo, Japan) and ultrasonically agitated using the Ceracon II (Shofu Inc.) (14). Then, the slurry was blotted with tissue to draw excess water. The specimens were then fired and cooled at one of the two cooling rates. All specimens were stored in water at 37°C for 24 h.

The specimens were then embedded in an acrylic resin (Unifast II, GC Corp., Tokyo, Japan) mold and mounted in a shear testing device (Tokyogiken Inc.) designed according to ISO TR 11405. To determine shear bond strength, a shear force was applied to the substrate/veneer interface using a mechanical testing device (Type 5567, Instron Corp., Canton, MA, USA) at a crosshead speed of 0.5 mm min⁻¹ until fracture.

The Kruskal-Wallis test was used to analyze differences in bond strength among the experimental groups, and the Mann-Whitney test was used for post-hoc comparisons. A *P* value of less than 0.05 was considered to indicate statistical significance. Some of the data have been previously published (14).

After shear testing, the fractured surfaces of specimens were observed with a stereomicroscope (Stemi DV4, Carl Zeiss MicroImaging GmbH, Göttingen, Germany) at an original magnification of ×32 to analyze the mode of failure, which was classified as adhesive failure at the veneering porcelain-ZrO₂ substrate interface (A), cohesive failure within the veneering porcelain (C), or combined adhesive/cohesive failure (AC). A scanning electron microscope (SEM; S-4300, Hitachi High-Technologies, Tokyo, Japan) was used to examine representative specimens after shear testing to clarify the failure mode. In addition, specimens of ZrO₂-EMX disks were embedded in acrylic resin (Unifast II, GC Corp.) and cut using a precision saw (Isomet Low Speed Saw, Buehler Ltd., Lake Bluff, IL, USA) equipped with a diamond wafering blade (15LC, Buehler Ltd.) to observe the interface of veneering porcelain and ZrO₂ material. After osmium coating with a sputter coater (HPC-IS, Vacuum Device Inc., Mito,

Japan) for 30 seconds, representative specimens were examined using the SEM at an acceleration voltage of 15 kV.

X-ray diffraction (XRD) analysis was undertaken to evaluate crystallization of the porcelain powder and to clarify the mode of failure. The veneering porcelain powder and specimen were examined after shear testing. Data were collected over an angular range from 3 degrees to 90 degrees 2θ (diffraction angle), with a step size of 0.04 and scan speed of 2 degrees min⁻¹. Cu Kα radiation was used (15 A and 30 kV). Data were analyzed using a diffractometer (MiniFlex II, Rigaku Corp. Tokyo, Japan) equipped with a graphite diffracted-beam monochromator (MiniFlex II, Rigaku Corp.).

Results

The shear bond strengths of the specimens are summarized in Table 3. Bond strength significantly differed by cooling time (0 vs 4 min) in the ZrO₂-AAA (*P* < 0.001) and ZrO₂-EMX (*P* = 0.001) specimens. In the ZrO₂-CZR specimens, shear bond strength did not significantly differ by cooling time (*P* = 0.382).

Table 4 shows the failure modes in specimens after shear bond testing. ZrO₂-AAA specimens cooled for 0 min suffered combined adhesive/cohesive failure. In ZrO₂-AAA specimens cooled for 4 min, the veneering porcelain spontaneously debonded from the ZrO₂ substrate. The ZrO₂-CZR and ZrO₂-EMX specimens suffered cohesive failures in the veneering porcelain at both cooling rates.

Figures 1A and 1B show SEM images of the interfaces between the veneering porcelain and ZrO₂ material in ZrO₂-EMX specimens cooled for 0 and 4 min, respectively. In Fig. 1A, numerous large porosities are present at the interface and in the veneering porcelain layer. In comparison, the porosities in Fig. 1B are considerably smaller in number and size. SEM images of the specimen surface after shear testing show that the entire surface of ZrO₂ was covered with veneering porcelain in EMX specimens cooled for 0 and 4 min (Figs. 2A and 2B).

The XRD patterns of CZR powder showed a number of peaks (namely 2θ = 16.69, 21.94, 26.13, and 27.44), and sanidine, lithium titanium niobium oxide, and orthoclase were identified (Fig. 3A). In contrast, the XRD

Table 3 Shear bond strength (MPa) between veneering porcelain (dentin/body) and ZrO₂

Veneering porcelain	Cooling time	Median	Mean	SD	Statistical category**
AAA	0	2.0*	1.8*	0.9*	a
AAA	4	0	0	0	b
CZR	0	28.4	27.5	3.1	c
CZR	4	27.2*	27.0*	4.0*	c
EMX	0	21.1*	22.1*	3.3*	d
EMX	4	29.2	27.5	2.7	c

See Table 1 for description of abbreviations.

* Quoted from reference #14.

** Identical letters indicate no statistically significant difference ($P > 0.05$).

Table 4 Mode of failure after shear bond testing

Veneering porcelain	Cooling time (min)	A	AC	C
AAA	0	0*	8*	0*
AAA	4	-	-	-
CZR	0	0	0	8
CZR	4	0*	0*	8*
EMX	0	0*	0*	8*
EMX	4	0	0	8

See Table 1 for description of abbreviations.

* Quoted from reference #14.

A: Adhesive failure at veneering porcelain-substrate interface;

AC: combined adhesive/cohesive failure;

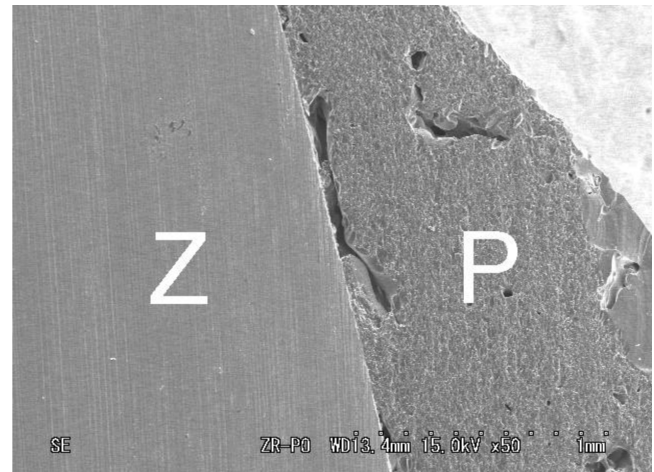
C: cohesive failure within veneering porcelain

patterns of EMX powder showed amorphous phases and no peak (Fig. 3B). The XRD patterns of representative specimens are shown in Fig. 4. An XRD pattern for cohesive failure after shear bond testing in EMX specimens cooled for 0 min shows a peak corresponding to SiO₂ (cristobalite; $2\theta = 20.96$; Fig. 4A). Figure 4B illustrates a typical XRD pattern for a ZrO₂ surface after airborne particle abrasion; no amorphous glass and no peak was found in the range of $2\theta = 15$ to 27 degrees.

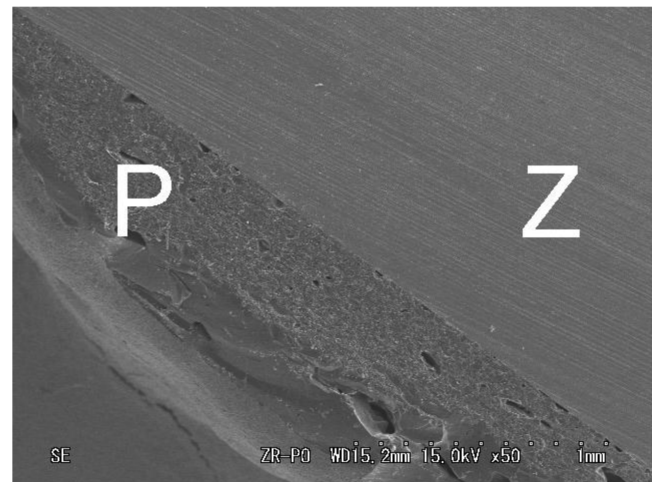
Discussion

The present study evaluated whether the rate of cooling from the firing temperature of porcelain affects shear bond strength between veneering porcelain and a zirconia material. The thermophysical properties of veneering porcelain and the cooling rate after firing can affect residual stress in veneering porcelain (15,16). Some studies showed that rapid cooling resulted in greater resistance to porcelain fracture in a metal-ceramic system (16). Moreover, rapid cooling was associated with the least crack propagation in an alumina-reinforced porcelain system (17). However, Guinn et al. (18) reported that slow cooling resulted in the highest bond strengths in porcelain-metal composite.

The results of the present study showed no significant difference in shear bond strength in CZR specimens cooled for 0 min (rapid cooling) or 4 min (slow cooling). In EMX specimens, however, slow cooling resulted in significantly



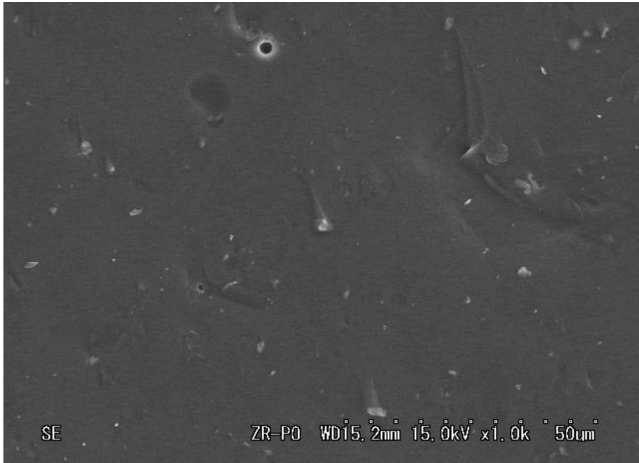
A



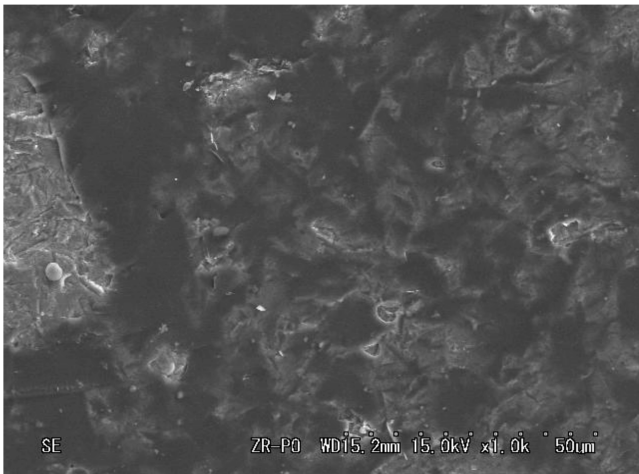
B

Fig. 1 SEM images (original magnification $\times 50$) of interface of veneering porcelain (IPS e.max Ceram) and ZrO₂ material. A: cooling time, 0 min; B: cooling time, 4 min. Z, ZrO₂ material; P, veneering porcelain.

higher shear bond strengths, as compared with rapid cooling. These results are presumably attributable to the composition of the veneering porcelain. XRD analysis



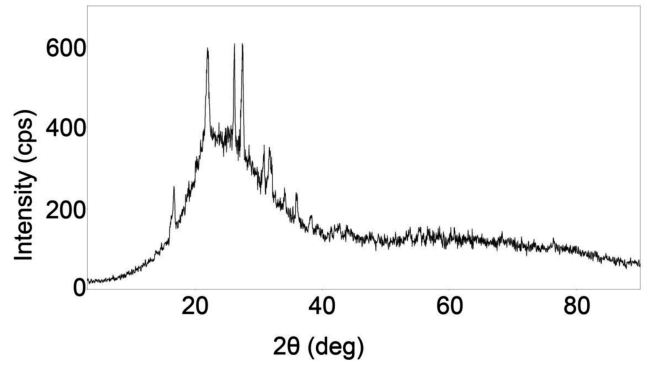
A



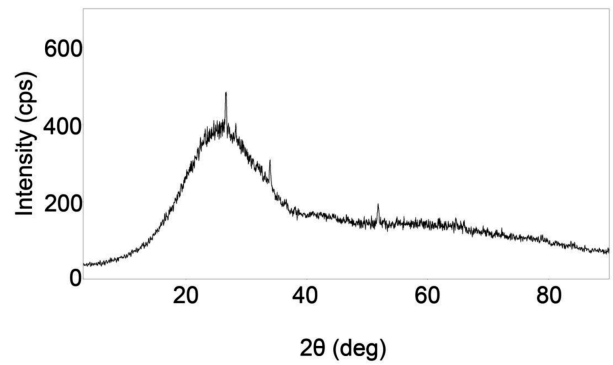
B

Fig. 2 SEM images (original magnification $\times 1,000$) of a ZrO_2 material surface of an EMX specimen after shear bond testing. A: cooling time, 0 min; B: cooling time, 4 min.

was used to detect the crystal phases of veneering porcelain compositions, and sanidine of feldspar, lithium titanium niobium oxide, and orthoclase were identified in CZR porcelain powder. In contrast, no peak or amorphous phase was observed in EMX porcelain powder. When fired porcelain is cooled to room temperature, the result is leucite particles embedded in a glass matrix. The indentation cracks in feldspathic porcelain are deflected away from leucite crystals (19). Microcracking from tensile stress during cooling of veneering porcelain reduces the susceptibility of the glassy matrix to fracture when the matrix contains leucite or mica crystal (20). Leucite is not a stable phase at ordinary porcelain firing temperature; however, sanidine, which has a lower thermal expansion than leucite, is the stable phase (21). Consequently, the shear



A



B

Fig. 3 XRD patterns of investigated porcelain powders. A: CZR porcelain powder, B: EMX porcelain powder.

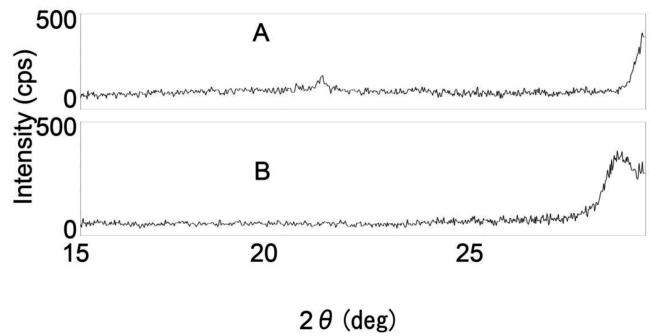


Fig. 4 XRD patterns of ZrO_2 surface. A: ZrO_2 -EMX specimen after shear bond testing, B: ZrO_2 surface after airborne particle abrasion.

bond strength of CZR porcelain to Katana zirconia material was not affected by the different cooling rates in the present study.

In EMX specimens, SEM images of the interfaces between the veneering porcelain and ZrO_2 material differed with respect to cooling rate. An SEM image after slow cooling (Fig. 1B) showed that the condition of the interface

between the EMX porcelain and Katana zirconia was superior to the state of the interface after rapid cooling (Fig. 1A). This difference may be related to the presence of crystallization in the veneer layer. Some veneering porcelains have components that promote crystallization, and strengthening of veneering porcelain might be related to crystallization and nucleation of the veneer layer. Veneering porcelain without such components could be unstable and more susceptible to variations in cooling rate. The findings of the present study suggest that, when applying EMX porcelain to a Katana zirconia material, slow cooling is recommended.

Within the limitations of the present study, it could be concluded that the time from firing temperature to room temperature may affect the shear bond strength between veneering porcelain and Katana zirconia material depending on porcelain material used. However, further studies are needed to examine the interactive effect of heating and cooling rates on both transient and residual stress states, and to reduce failures in core-veneered zirconia-based restorations.

Acknowledgments

This study was supported in part by a Grant-in-Aid for Scientific Research (C 20592288) from the Japan Society for the Promotion of Science (JSPS) and a grant from the Promotion and Mutual Aid Corporation for Private Schools of Japan (2009 and 2010).

References

- Christensen GJ (1999) Porcelain-fused-to-metal vs. nonmetal crowns. *J Am Dent Assoc* 130, 409-411.
- Blatz MB (2002) Long-term clinical success of all-ceramic posterior restorations. *Quintessence Int* 33, 415-426.
- Vult von Steyern P, Carlson P, Nilner K (2005) All-ceramic fixed partial dentures designed according to the DC-Zirkon technique. A 2-year clinical study. *J Oral Rehabil* 32, 180-187.
- Raigrodski AJ, Chiche GJ, Potiket N, Hochstedler JL, Mohamed SE, Billiot S, Mercante DE (2006) The efficacy of posterior three-unit zirconium-oxide-based ceramic fixed partial dental prostheses: a prospective clinical pilot study. *J Prosthet Dent* 96, 237-244.
- Sailer I, Fehér A, Filser F, Gauckler LJ, Lüthy H, Hämmerle CH (2007) Five-year clinical results of zirconia frameworks for posterior fixed partial dentures. *Int J Prosthodont* 20, 383-388.
- Roediger M, Gersdorff N, Huels A, Rinke S (2010) Prospective evaluation of zirconia posterior fixed partial dentures: four-year clinical results. *Int J Prosthodont* 23, 141-148.
- Aboushelib MN, de Jager N, Kleverlaan CJ, Feilzer AJ (2005) Microtensile bond strength of different components of core veneered all-ceramic restorations. *Dent Mater* 21, 984-991.
- Anusavice KJ, Hojjatie B (1992) Tensile stress in glass-ceramic crowns: effect of flaws and cement voids. *Int J Prosthodont* 5, 351-358.
- Ritter JE (1995) Critique of test methods for lifetime predictions. *Dent Mater* 11, 147-151.
- Tuccillo JJ, Nielsen JP (1972) Shear stress measurements at a dental porcelain-gold bond interface. *J Dent Res* 51, 626-633.
- Bertolotti RL (1980) Calculation of interfacial stress in porcelain-fused-to-metal systems. *J Dent Res* 59, 1972-1977.
- Shell JS, Nielsen JP (1962) Study of the bond between gold alloys and porcelain. *J Dent Res* 41, 1424-1437.
- Göstemeyer G, Jendras M, Dittmer MP, Bach FW, Stiesch M, Kohorst P (2010) Influence of cooling rate on zirconia/veneer interfacial adhesion. *Acta Biomater* 6, 4532-4538.
- Saito A, Komine F, Blatz MB, Matsumura H (2010) A comparison of bond strength of layered veneering porcelains to zirconia and metal. *J Prosthet Dent* 104, 247-257.
- Asaoka K, Tesk JA (1989) Transient and residual stresses in dental porcelains as affected by cooling rates. *Dent Mater J* 8, 9-25.
- Dehoff PH, Anusavice KJ (1989) Tempering stresses in feldspathic porcelain. *J Dent Res* 68, 134-138.
- Baharav H, Laufer BZ, Mizrahi A, Cardash HS (1996) Effect of different cooling rates on fracture toughness and microhardness of a glazed alumina reinforced porcelain. *J Prosthet Dent* 76, 19-22.
- Guinn JW 3rd, Griswold WH, Vermilyea SG (1982) The effect of cooling rate on the apparent bond strength of porcelain-metal couples. *J Prosthet Dent* 48, 551-554.
- Morena R, Lockwood PE, Fairhurst CW (1986) Fracture toughness of commercial dental porcelains. *Dent Mater* 2, 58-62.
- Cattell MJ, Knowles JC, Clarke RL, Lynch E (1999) The biaxial flexural strength of two pressable ceramic systems. *J Dent* 27, 183-196.
- Mackert JR Jr, Evans AL (1991) Effect of cooling rate on leucite volume fraction in dental porcelains. *J Dent Res* 70, 137-139.